Estimation of Mutual Induction Eddy Current Testing Method Using Horizontal Exciting Coil and Spiral Search Coil

Tatsuya Marumoto[1(✉)], Yuta Motoyasu[1], Yuji Gotoh[1], and Tatsuo Hiroshima[2]

[1] Oita University, 700 Dannoharu, Oita 870-1192, Japan
`Marupa.com@gmail.com`
[2] Hokuto Electronics, INC., 2-36, Najiotoukubo, Nishinomiya, Hyogo 669-1148, Japan

Abstract. The mutual induction type eddy current testing using a spiral type search coil is one of the eddy current testing (ECT). In this type ECT probe, since the thickness of a spiral search coil is very thin, the distance (lift-off: L_o) between the ECT probe and the specimen is able to set small. Therefore, the high detection sensitivity is obtained. However, since the wire is coiled in the shape of spiral, the evaluation of the flux density inside the spiral search coil is made difficult by experiment. Moreover, the phenomenon elucidation of inspection using this ECT probe is not carried out. In this paper, the inspection characteristic of a surface defect on an aluminum plate using this probe was investigated by 3-D alternating electromagnetic finite element method (FEM). Moreover, the evaluation in consideration of the characteristic of the spiral search coil in this ECT probe is also investigated by (1 + 1) evolution strategy. It is shown that high detection sensitivity is obtained using the spiral search coil.

Keywords: Mutual induction type eddy current testing · Spiral search coil · (1 + 1) evolution strategy · 3-D FEM

1 Introduction

The eddy current testing (ECT) is one of the electromagnetic inspection methods [1, 2] of surface defect in a non-magnetic material, etc. There are a self-induction type and a mutual induction type in the ECT. In the self-induction type, the exciting current is passed to one coil and the impedance of the coil is measured. As for this type, both excitation and detection are carried out with one coil. Since it is necessary to make the coil small when detecting small defect using this type, it is made difficult to enlarge the exciting current. As for the mutual induction type, the exciting coil and the search coil have been independent, respectively. Therefore, a large magnetic field is able to impress to the specimen using this type.

In order to increase the detection sensitivity of the defect in the specimen using the mutual induction type, it is necessary to decrease the distance (lift-off: Lo) between the ECT probe and the specimen [3]. In recent years, the manufacture technology of a semiconductor was applied, and the spiral search coil film in the ECT probe was

created. Since the thickness of the spiral coil is very thin, the Lo is able to set small. However, since the wire is coiled in the shape of spiral, the evaluation of the flux density inside the spiral search coil is made difficult by experiment. Moreover, the phenomenon elucidation of the ECT probe using the spiral search coil is not carried out.

In this paper, the inspection principle of the mutual induction type ECT probe using the spiral search coil was investigated by 3D electromagnetic finite element method (FEM). Moreover, the measured flux density inside the spiral search coil is calculated by the inversion method using the (1 + 1) evolution strategy [4–6], and it is compared with the calculated result of 3D FEM.

2   Procedure for Paper Submission

2.1   Inspection Model

Figure 1 shows the inspection model of 1/2 domain of the ECT probe using a spiral search coil. The structure is a rectangle exciting coil and a spiral search coil. The impression magnetic field by the exciting coil is distributed in the x-directions. The diameter, the thickness and number of turns of the spiral search coil are 2 mm, 0.1 mm and 44 turns, respectively. As for the search coil, the z-direction flux density (Bz) on the surface of specimen is detected. An aluminum plate of specimen is magnetized by exciting coil of 25 kHz and 4.6 A-turns. The distance (lift-off: Lo) from the bottom of the spiral search coil to the surface of the aluminum plate is equal to 1 mm. In this research, since the elucidation of the inspection principle of this ECT is the main purposes, the size of a defect is set as rectangular large dimensions as shown in Fig. 1.
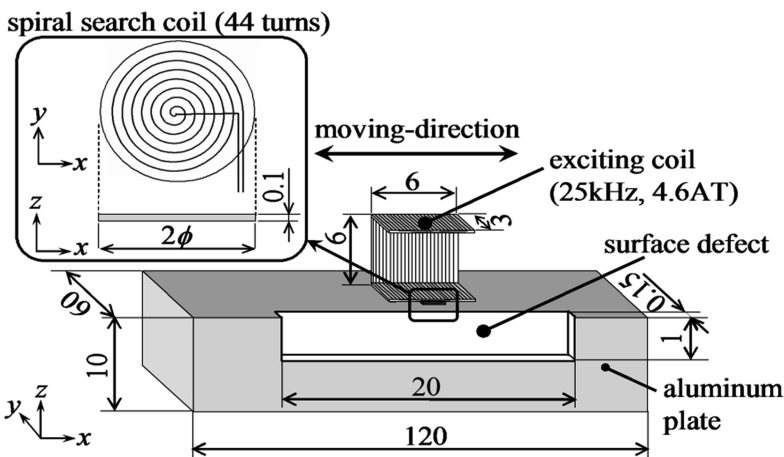
Fig. 1. Inspection model for surface defect on aluminum plate (1/2domain).

This ECT probe is moved in the x-direction on the aluminum plate, and the surface defect is inspected. The conductivity of the aluminum specimen is 3.5×10^7 S/m.

2.2   3-D Electromagnetic FEM Analysis

3-D FEM using the 1st order hexahedral edge element is applied. The flux density is analyzed by the step-by-step method taking account of eddy current in the aluminum plate. In order to get the steady state result, the calculation is carried out during 3 periods (=96steps). The time interval $\varDelta t$ of the step-by-step method is chosen as 1.25×10^{-6} s.

The basic equation of eddy current analysis using the A-ϕ method is given by

$$rot(v\,rot\,A) = J_o - \sigma\left(\frac{\partial A}{\partial t} + grad\varphi\right) \tag{1}$$

$$div\left\{-\sigma\left(\frac{\partial A}{\partial t} + grad\,\phi\right)\right\} = 0 \tag{2}$$

where A is the magnetic vector potential, ϕ is the scalar potential, v is the reluctivity, J_o is the current density and σ is the conductivity.

3   Elucidation of Inspection Principle

The elucidation of the inspection principle of this ECT probe is carried out using this 3-D FEM. Figure 2 shows the distribution of calculated Bz in the spiral search coil by moving the ECT probe in the x-direction on the aluminum plate with surface defect. The Bz is displayed on plus, when the waveform of both exciting current and Bz in the search coil is same phase. And it is displayed on minus when the phase is reverse. The figure denotes that each peak value is obtained near two edges of the defect. Therefore, a surface defect is detectable from these two peak values.

Figure 3 shows the distribution of magnetic flux near a surface defect when the ECT probe is located at the centre (x = 0 mm) of the defect as shown in Fig. 2. This figure illustrates that the impression magnetic field from an exciting coil is distributed in the about x-directions. Figure 4 shows only z-component of magnetic flux near a surface defect. These figures denotes that since the plus and minus values of z-component of the flux inside a search coil are almost equal, the output voltage is hardly generated by a search coil.

Figure 5 shows the distribution of magnetic flux near a surface defect when the ECT probe is located in the edge part (x = 9.5 mm) of the defect as shown in Fig. 2. Then, Fig. 6 shows the distribution of eddy current density near a surface defect inside the aluminium plate. Figure 6(a) shows the distribution of eddy current inside the aluminium plate in x-z plane. And, Fig. 6(b) shows the vector distribution of eddy current surface inside the aluminium plate in x−y plane. Figure 5 illustrates that the impressed magnetic field is hardly distributed inside the aluminium plate near the edge part of a
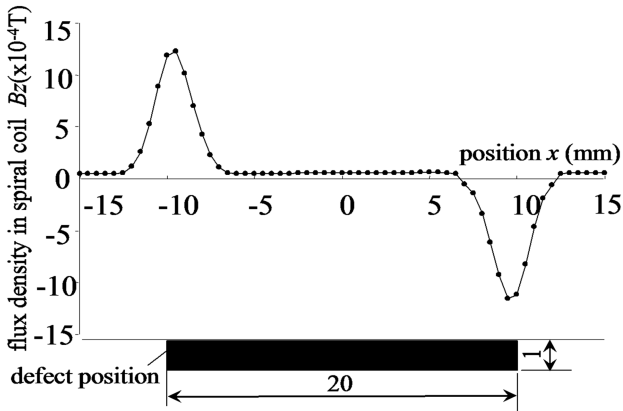
Fig. 2. Inspection waveform of flux density Bz (calculated, 25 kHz, 4.6 AT)
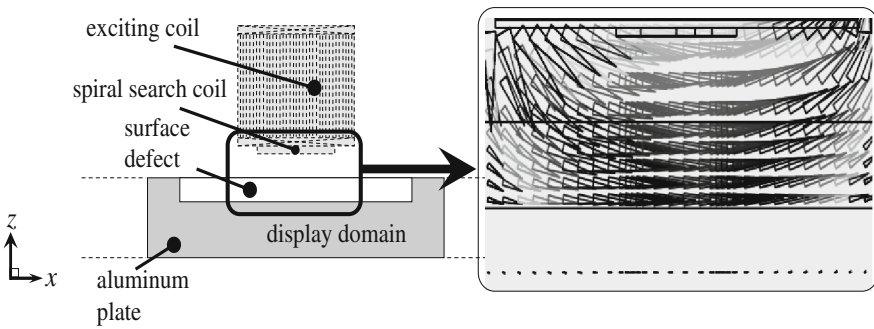
Fig. 3. Distribution of magnetic flux near a surface defect when the ECT probe is located in the centre of the defect ($B_{max} = 5.98 \times 10^{-4}$T).
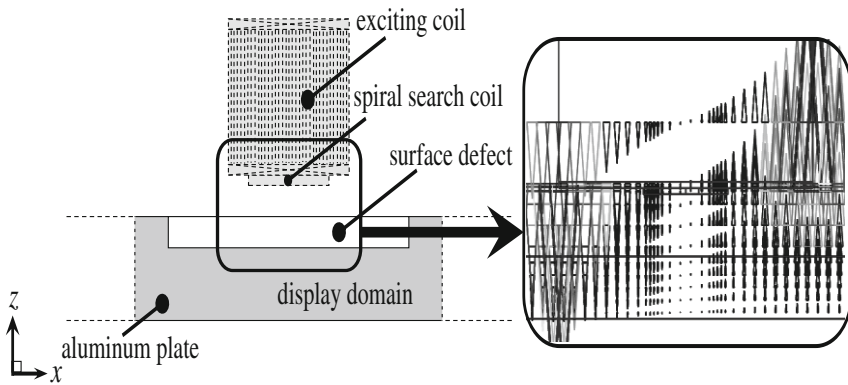
Fig. 4. Distribution of z-component of magnetic flux near a surface defect when the ECT probe is located in the centre of the defect.
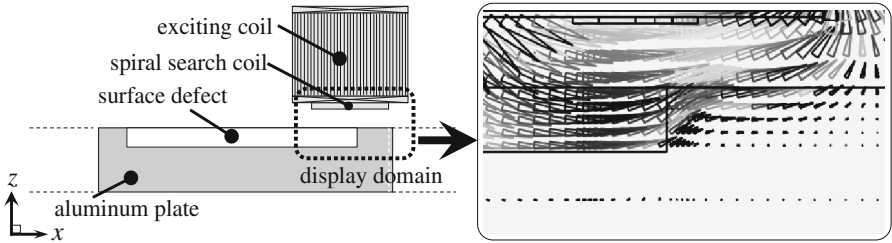
Fig. 5. Distribution of magnetic flux near a surface defect when the ECT probe is located in the edge part of the defect ($B_{max} = 6.16 \times 10^{-4}$T).
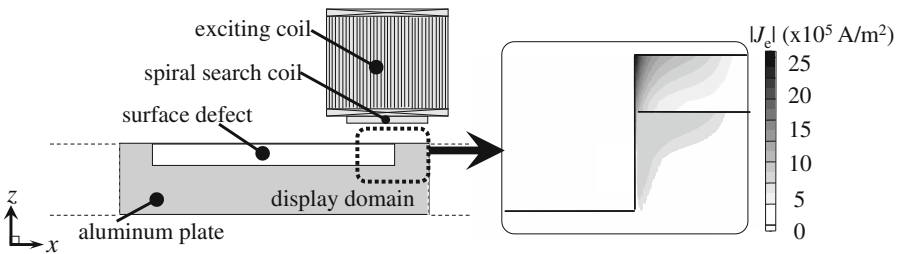
(a) *x-z* plane
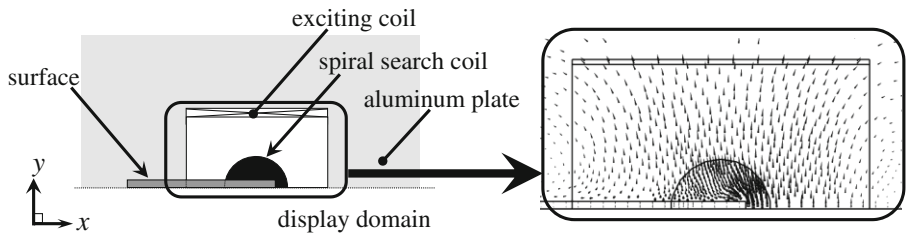
(b) x-y plane

Fig. 6. Distribution of eddy current near a surface defect when the ECT probe is located in the edge part of the defect.

defect, and is bypassed to z-direction. This is, because the eddy current is generated inside the edge portion as shown in Fig. 6. Figure 7 shows only z-component of magnetic flux near a surface defect. This figure denotes that the z-component of flux near the edge part of the defect is strongly distributed, since the eddy current is distributed inside the aluminum plate near the edge of defect. Therefore, the output voltage is generated by a search coil near this position.

4 Evaluation for Detecting Surface Defect

4.1 Output Signal Analysis Using Evolution Strategy

The comparison with verification experiment and calculation by 3D FEM is evaluated by flux density inside the spiral search coil (44 turns) in the ECT probe. In the verification experiment, since the shape of the search coil is spiral, the conversion to flux density from the output voltage Ve of the search coil is difficult. In this research, the spiral search coil is assumed to be the coils with 44 kinds of diameter as shown in Fig. 8. Then, the measured flux density inside the spiral search coil is calculated by the (1 + 1) evolution strategy. Various techniques are proposed for solving the inverse problem. Although large number of calculations is necessary in the (1 + 1) evolution strategy, it is adopted because a global optimal solution can be obtained.

The iteration process of calculation is as follows:

(1) Calculation of output voltage in the spiral search coil
The flux density Bz inside 44 kinds of diameter of the search coils is chosen as design variable. Then, total output voltage Vc is calculated. The formula of flux density Bz inside each diameter using random number, and total output voltage Vc are given by

$$B_z^n = B_z^n + N(0, \sigma^2) \quad (n = 1,\ 2,\ 3, \ldots,\ 44) \tag{3}$$

$$V_c^n = -S^n \frac{dB_z^n}{dt} \quad (n = 1,\ 2,\ 3, \ldots, 44) \tag{4}$$

$$V_c = \sum_{n=1}^{44} V_c^n \tag{5}$$

where, B_z^n is flux density of z-direction inside the n-th diameter of the spiral search coil, $N(0, \sigma^2)$ (σ: standard deviation) is the normal random number with weight value, S^n is the n-th cross-section area (m^2) in the spiral search coil, and V_c is calculated output voltage in total spiral search coil. The normal random number $N(0, \sigma^2)$ with weight value is added to each flux density in 44 kinds of coils. And the total output voltage of the spiral search coil is calculated from the sum total of the output voltage inside each diameter.

(2) Calculation of objective function
The following objective function W is calculated by

$$W = |V_c - V_e| \tag{6}$$

where, Vc is calculated output voltage and Ve is measured output voltage in the spiral search coil. The residual of the measured output voltage Ve and the calculated output voltage Vc is an objective function W. If the calculated objective function W is less than the previous one, W is updated. The initial value of the standard deviation σ and the convergence criterion of the objective function W are 2.25 and 1×10^{-3} mV, respectively.
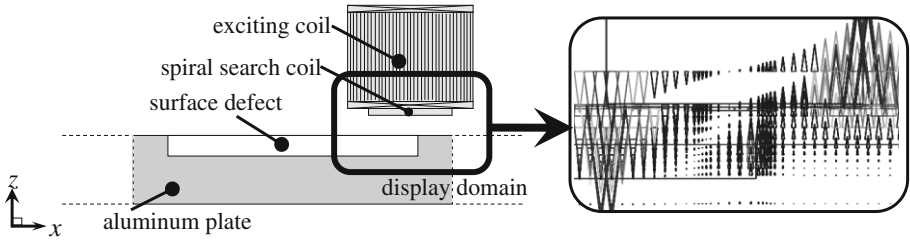
Fig. 7. Distribution of z-component of magnetic flux near a surface defect when the ECT probe is located in the edge part of the defect.

Above process is iterated until the final result is obtained. Then, the final flux density Bz in the spiral search coil is calculated by

$$B_z = \sum_{n=1}^{44} B_z^n \qquad (7)$$

Where, Bzn is flux density of z-direction inside the n-th diameter of the spiral search coil and Bz is final flux density of z-direction in the spiral search coil.
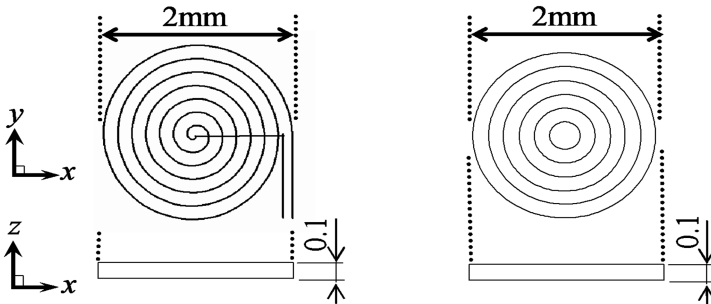
Fig. 8. Spiral search coil (44 turns) and assumed coils with 44 kinds of diameter.

4.2 Inspection of Surface Defect

Figure 9 shows the distribution of calculated and measured values of Bz in the spiral search coil. The calculated result Bz by 3D FEM is shown in the "calculated (△)" inside this figure. And, the "measured (◆)" in this figure is the value which changed measured output voltage Ve into flux density Bz using the (1 + 1) evolution strategy. Bz is obtained by moving the ECT probe in the x-direction on the aluminum plate. The figure denotes that each peak value is obtained near two edges of the defect. Figures 10 and 11 show the distribution of calculated and measured values of Bz in the spiral search coil when the lengths of x-direction of the surface defect are set to 10 mm and 5 mm, respectively. The width of y-direction and the depth of z-direction of these
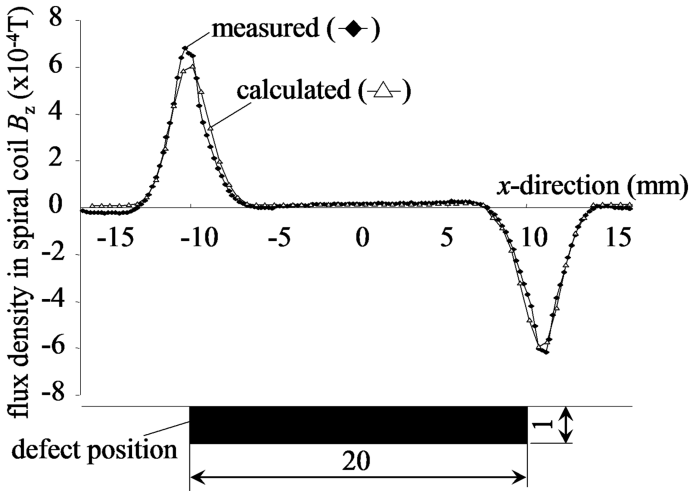
Fig. 9. Distribution of calculated and measured values of B_z in the spiral search coil (25 kHz, 4.6 AT).
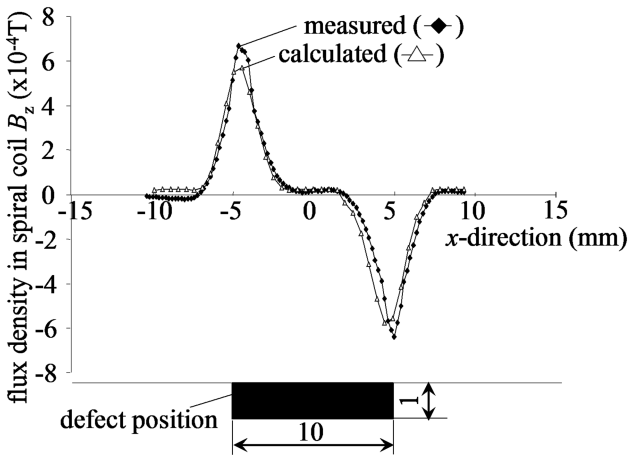
Fig. 10. Distribution of calculated and measured values of B_z in the spiral search coil when the length of the surface defect is 10 mm (25 kHz, 4.6 AT).

defects are same dimensions, and are 0.3 mm and 1 mm, respectively. These figures denote that the length of x-direction of the surface defect is presumed from the distance between each peak value of Bz. However, even if the length of x-direction of the surface defect is changed, the amplitude of each peak value of Bz is not almost changed. The calculated results are in agreement with measurement.
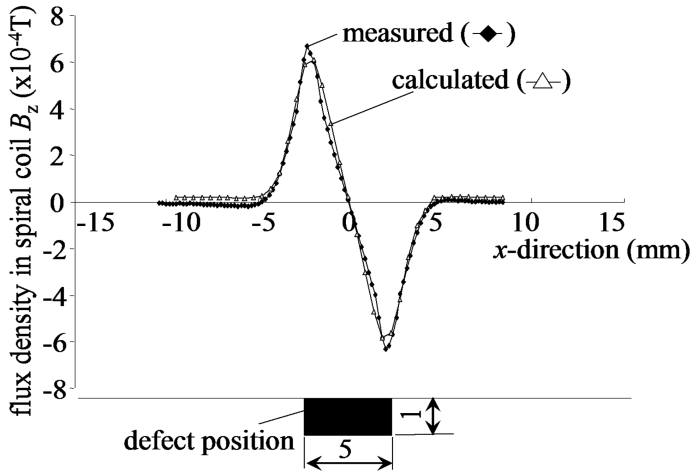
Fig. 11. Distribution of calculated and measured values of B_z in the spiral search coil when the length of the surface defect is 5 mm (25 kHz, 4.6 AT).

4.3   Effect of Spiral Search Coil

In this research, the comparison of the detecting sensitivity of a usual search coil and a spiral search coil in this ECT probe is investigated by 3D FEM. The diameter, the thickness and number of turns of the usual search coil are the same as the spiral coil, and are 2 mm, 0.1 mm and 44 turns, respectively. The structure of the usual coil is that the wire is rolled 44 times with the same diameter of 2 mm as shown in Fig. 12. Figure 13 shows the calculated Bz in the spiral search coil and usual search coil. The figure denotes that each peak value near two edges of the defect by the spiral coil is higher than that by the usual search coil. In the usual search coil, the average value of the magnetic flux distributed inside of the search coil is detected. On the other hand, in the spiral search coil, total value of the intensity distribution of the magnetic flux inside the coil is detected. Therefore, the flux detection sensitivity of the spiral coil is higher than that of the usual search coil.
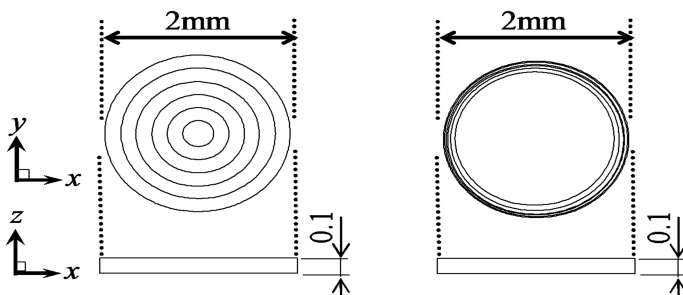
Fig. 12. Model of spiral search coil and usual search coil (diameter: 2 mm, thickness: 0.1 mm, 44 turns).
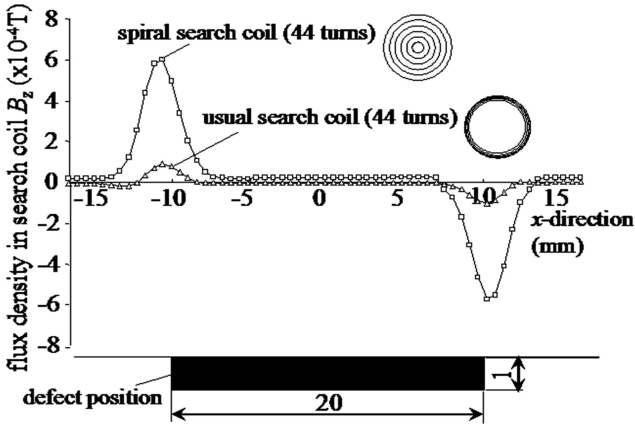
Fig. 13. Inspection signal waveform of calculated values of *Bz* in the spiral search coil and usual search coil (calculated, 25 kHz, 6.51 AT).

5   Conclusions

The results obtained are summarized as follows:

(1) In this mutual induction ECT probe, the impressed magnetic field is distributed to bypass the edge portion of the surface defect, since eddy current is generated inside the aluminum plate near the edge portion of the defect. Therefore, output signal in the search coil is obtained near two edges of the defect.

(2) It is possible to estimate the magnetic flux density from measured output voltage in the spiral search coil of this ECT probe using evolution strategy. Moreover, it is shown that the detection sensitivity of the spiral search coil is higher than that of the usual search coil.

The investigation of the detectable size and form of the defect by this inspection method is a future subject.

References

1. Goldfine, N.J.: Magnetometers for improved materials characterization in aerospace applications. Mater. Eval. **51**, 396–405 (1993). The American Society for Nondestructive Testing
2. McMaster, R.C., Mclntrire, P., Mester, M.L.: Electromagnetic Testing. Nondestructive Testing Handbook, vol. 5, 3edn. American Society for Nondestructive Testing (2004)
3. Gotoh, Y., Matsuoka, A., Takahashi, N.: Electromagnetic inspection technique of thickness of nickel-layer on steel plate without influence of lift-off between steel and inspection probe. IEEE Trans. Magn. **47**(5), 950–953 (2011)
4. Bäck, T.: Evolutionary Algorithms in Theory and Practice. Oxford University Press, Oxford (1996)

5. Horii, M., Takahashi, N., Narita, T.: Investigation of evolution strategy and optimization of induction heating model. IEEE Trans. Magn. **36**(4), 1085–1088 (2000)
6. Gotoh, Y., Fujioka, H., Takahashi, N.: Proposal of electromagnetic inspection method of outer side defect on steel tube with steel support plate using optimal differential search coils. IEEE Trans. Magn. **47**(5), 1006–1009 (2011)